EUROPEAN ORGANIZATION FOR NUCLEAR RESEARCH

arXiv:2308.16131v2 [nucl-ex] 2 Sep 2023

Observation of medium-induced yield enhancement and acoplanarity broadening of low-p_T jets from measurements in pp and central Pb–Pb collisions at $\sqrt{s_{NN}} = 5.02$ TeV

ALICE Collaboration*

Abstract

The ALICE Collaboration reports the measurement of semi-inclusive distributions of charged-particle jets recoiling from a high transverse momentum (high p_T) hadron trigger in proton–proton and central Pb–Pb collisions at $\sqrt{s_{NN}} = 5.02$ TeV. A data-driven statistical method is used to mitigate the large uncorrelated background in central Pb–Pb collisions. Recoil jet distributions are reported for jet resolution parameter $R = 0.2$, 0.4, and 0.5 in the range $7 < p_{T,jet} < 140$ GeV/c and trigger–recoil jet azimuthal separation $\pi/2 < \Delta\varphi < \pi$. The measurements exhibit a marked medium-induced jet yield enhancement at low p_T and at large azimuthal deviation from $\Delta\varphi \sim \pi$. The enhancement is characterized by its dependence on $\Delta\varphi$, which has a slope that differs from zero by 4.7σ. Comparisons to model calculations incorporating different formulations of jet quenching are reported. These comparisons indicate that the observed yield enhancement arises from the response of the QGP medium to jet propagation.

*See Appendix A for the list of collaboration members

Matter at very high temperature or pressure forms a quark–gluon plasma (QGP), the state of matter in which quarks and gluons are not bound in colorless hadrons [1, 2]. A QGP filled the early universe a few microseconds after the Big Bang, and is generated in the laboratory today in high-energy collisions of atomic nuclei at the Large Hadron Collider (LHC) and the Relativistic Heavy Ion Collider (RHIC) [3–7]. Comparison of measurements at these facilities with theoretical model calculations shows that the QGP exhibits emergent collective behavior, flowing with very low specific shear viscosity [8]. Calculations using finite-temperature quantum chromodynamics (QCD) on the lattice demonstrate that, at temperatures several times the transition temperature of about 150 MeV from hadronic matter to the QGP, the effective number of degrees of freedom of the QGP is ∼15% lower than that expected for freely-interacting quarks and gluons at asymptotically high temperature [9, 10]. However, detailed understanding of the origin of these emergent collective phenomena in terms of quasi-particle degrees of freedom and their interactions remains elusive.

In high-energy hadronic collisions, QCD jets are generated by the hard (high momentum transfer Q^2) scattering of quarks and gluons (partons) from the colliding projectiles. The scattered partons are initially virtual and evolve by radiating a parton shower, which hadronizes into a correlated spray of colorless hadrons that is experimentally observable. In proton–proton (pp) collisions, measurements of inclusive jet production provide stringent tests of high-order perturbative QCD (pQCD) calculations [11–13]. In nucleus–nucleus (A–A) collisions, the hard-scattered partons and their showers interact with the QGP as it expands and cools, which modifies jet production rates and internal jet structure relative to that in pp collisions ("jet quenching") [14]. Comparisons of jet quenching measurements with theoretical calculations provide unique insight into the dynamics and transport properties of the QGP [15, 16].

Measurements of medium-induced jet angular deflection and modification of jet substructure have been proposed to elucidate the microscopic structure of the QGP [17–19]. Jet scattering off QGP quasi-particles is the partonic analog to Rutherford scattering of α particles, which revealed the existence of the atomic nucleus [20]. However, such jet deflection measurements are challenging in the heavy-ion collision environment, due to the large and complex uncorrelated background. This is especially the case for jets with low transverse momentum ($p_{\mathrm{T,jet}}$), for which deflection effects may be sizable.

In this Letter the ALICE Collaboration reports measurements of the semi-inclusive distribution of charged-particle jets recoiling from a high-p_{T} hadron trigger [21, 22] in inelastic pp and in central Pb–Pb collisions at center-of-mass energy per nucleon–nucleon collision $\sqrt{s_{\mathrm{NN}}} = 5.02$ TeV. The uncorrelated background jet yield in central Pb–Pb collisions is corrected using the trigger p_{T}-differential statistical approach developed in Ref. [22]. This approach enables precise measurements of recoil jet distributions at low $p_{\mathrm{T,jet}}$ and large jet radius R in central A–A collisions, which is necessary in a search for jet deflection effects over broad phase space.

Recoil jet yield distributions are measured as a function of $p_{\mathrm{T,jet}}$ and acoplanarity $\Delta\varphi$, the azimuthal separation of the trigger hadron and recoil jet, for jet resolution parameters $R = 0.2$, 0.4, and 0.5. As a function of $p_{\mathrm{T,jet}}$, measurements are reported in the range $7 < p_{\mathrm{T,jet}} < 140$ GeV/c for recoil jets in the range $|\Delta\varphi - \pi| < 0.6$. As a function of $\Delta\varphi$, measurements are reported in the range $\pi/2 < \Delta\varphi < \pi$, in $p_{\mathrm{T,jet}}$ intervals between 10 and 100 GeV/c.

The comparison of distributions measured in pp and central Pb–Pb collisions reveals a marked medium-induced enhancement at $\Delta\varphi$ values far from π, for low $p_{\mathrm{T,jet}}$ and large R. The systematic dependence of this enhancement on $p_{\mathrm{T,jet}}$ and R is discussed in terms both of jet–medium scattering and of the response of the QGP medium to jet energy loss. Theoretical calculations incorporating different implementations of jet quenching are compared to the data. These comparisons provide strong discrimination between the models, favoring medium response as the origin of the observed enhancement. Details of the analysis, together with additional physics results, are reported in a companion article [23].

The ALICE apparatus and its performance are described in Refs. [24, 25]. The data for pp collisions

at $\sqrt{s} = 5.02$ TeV were recorded during the 2015 and 2017 LHC runs using a minimum bias (MB) trigger [23]. The data for Pb–Pb collisions at $\sqrt{s_{\mathrm{NN}}} = 5.02$ TeV were recorded during the 2018 run using MB and centrality-enhanced triggers [23]. The Pb–Pb event population with highest event activity in the forward V0 detectors is selected, corresponding to the 10% most-central fraction of the total Pb–Pb hadronic interaction cross section. After offline event selection, the dataset for analysis has 1.04B events for pp collisions and 89M events for central Pb–Pb collisions.

Charged-particle tracks are reconstructed from hits in the ALICE Inner Tracking System (ITS) and Time Projection Chamber (TPC). The response of these detectors was non-uniform in azimuth and varied between data-taking runs. Tracks are selected to account for such variations, in order to achieve uniform and stable tracking efficiency [23]. Tracks are accepted within pseudorapidity $|\eta| < 0.9$ and $p_{\mathrm{T}} > 0.15$ GeV/c.

The same analysis is carried out on pp and central Pb–Pb events. Events are selected based on the presence of a high-p_{T} charged-hadron trigger track within $p_{\mathrm{T,low}} < p_{\mathrm{T}} < p_{\mathrm{T,high}}$, denoted TT$\{p_{\mathrm{T,low}}, p_{\mathrm{T,high}}\}$ ("Trigger Track," units in GeV/c). If an event includes multiple particles satisfying the trigger condition, one such particle is chosen at random as the trigger. The p_{T}-dependence of the resulting TT distribution corresponds to that of inclusive charged-particle production. The analysis utilizes two TT classes, TT$\{20, 50\}$, denoted "signal", and TT$\{5, 7\}$, denoted "reference."

For TT-selected events, jet reconstruction with charged tracks is carried out in two passes, using the k_{T} and anti-k_{T} jet reconstruction algorithms and the p_{T} recombination scheme [26–28]. The jet acceptance is $|\eta_{\mathrm{jet}}| < 0.9 - R$ over the full azimuth, with additional selection on jet area to suppress unphysical jets [21]. Jets containing tracks with $p_{\mathrm{T}} > 100$ GeV/c are rejected due to limited track momentum resolution in that range; this selection has negligible effect on the reported results. There is no other rejection of individual jet candidates in the analysis.

The first reconstruction pass utilizes the k_{T} algorithm to estimate the event-wise median p_{T} density ρ [21, 29]. The signal and reference TT-selected event populations have different distributions of hard jets, which in Pb–Pb collisions generates a small misalignment of the ρ distribution of the signal and reference populations [22, 23]. To enable precise subtraction of the uncorrelated background yield, the reference-TT ρ distribution is shifted relative to that of signal-TT events by a constant value $\Delta\rho$ which is optimized using a data-driven procedure, finding $\Delta\rho = 1.7 \pm 0.1$ GeV/c, i.e. a $\sim 1\%$ correction to ρ that is determined with sub-per mil precision. This shift markedly improves the precision of the uncorrelated jet background correction at low $p_{\mathrm{T,jet}}$ [22, 23]. In pp collisions this shift is negligible so a similar correction is not required.

The second reconstruction pass generates the jet population for physics analysis, utilizing the anti-k_{T} algorithm with $R = 0.2$, 0.4, and 0.5. The p_{T} of each second-pass jet is adjusted for the background density ρ via $p_{\mathrm{T,ch\ jet}}^{\mathrm{reco},i} = p_{\mathrm{T,ch\ jet}}^{\mathrm{raw},i} - \rho A_{\mathrm{jet}}^{i}$ [29], where $p_{\mathrm{T,ch\ jet}}^{\mathrm{raw},i}$ is the raw p_{T} of jet i in the event and A_{jet}^{i} is its area, and "ch" denotes charged-particle jets.

The distributions of recoil jets in $(p_{\mathrm{T,ch\ jet}}, \Delta\varphi)$ for the signal-TT and reference-TT datasets are normalized by the corresponding number of trigger hadrons. Since the p_{T}-distribution of the TT population corresponds to that of inclusive hadron production, the normalized distributions are semi-inclusive; in the absence of uncorrelated background they are equivalent to the ratio of the production cross sections of trigger hadron–recoil jet coincidences and inclusive trigger hadrons [21].

The observable Δ_{recoil} is defined as the difference of the trigger-normalized signal-TT and reference-TT distributions [21]:

$$\Delta_{\mathrm{recoil}}(p_{\mathrm{T,jet}}, \Delta\varphi) = \frac{1}{N_{\mathrm{trig}}} \frac{\mathrm{d}^2 N_{\mathrm{jet}}}{\mathrm{d}p_{\mathrm{T,jet}} \mathrm{d}\Delta\varphi} \bigg|_{p_{\mathrm{T}}^{\mathrm{trig}} \in \mathrm{TT_{sig}}} - c_{\mathrm{Ref}} \times \frac{1}{N_{\mathrm{trig}}} \frac{\mathrm{d}^2 N_{\mathrm{jet}}}{\mathrm{d}p_{\mathrm{T,jet}} \mathrm{d}\Delta\varphi} \bigg|_{p_{\mathrm{T}}^{\mathrm{trig}} \in \mathrm{TT_{ref}}} . \quad (1)$$

3

The scale factor c_{Ref} is extracted from data as discussed below. The reference distribution in the second term includes an admixture of trigger-correlated yield, so that $\Delta_{\mathrm{recoil}}(p_{\mathrm{T,jet}}, \Delta\varphi)$ is not directly interpretable as the semi-inclusive distribution for the signal-TT population except in the high-$p_{\mathrm{T,ch\ jet}}^{\mathrm{reco}}$ tail [21, 23]. Nevertheless, both terms are perturbatively calculable, and this observable provides precise, data-driven correction for the large uncorrelated yield at low $p_{\mathrm{T,jet}}$ and large R.

Both terms in Eq. (1) include a significant yield of jet candidates that are not correlated with the trigger hadron, and whose $p_{\mathrm{T,jet}}$ distributions are therefore identical in the signal and reference TT-selected populations. Because ρ is the median local p_{T}-density, approximately half of the jet yield has $p_{\mathrm{T,ch\ jet}}^{\mathrm{reco}} < 0$; the yield in this region is expected to be dominated by jet candidates that are not correlated with the trigger. Indeed, the shapes of the signal-TT and reference-TT (or its equivalent) recoil jet distributions in the negative-most region of $p_{\mathrm{T,ch\ jet}}^{\mathrm{reco}}$ are found to be consistent within uncertainties in central A–A collisions, thereby validating this picture [21–23].

However, the magnitudes of the signal-TT and reference-TT trigger-normalized distributions differ in the negative-most region of $p_{\mathrm{T,ch\ jet}}^{\mathrm{reco}}$, due to conservation of jet number density in high-multiplicity events and the larger population of hard jets at large positive $p_{\mathrm{T,ch\ jet}}^{\mathrm{reco}}$ for the signal-TT population (i.e. higher $p_{\mathrm{T}}^{\mathrm{trig}}$ generates a harder recoil jet spectrum) [21–23, 30]. The factor c_{Ref} accounts for this effect by normalizing the reference-TT to the signal-TT distribution in the negative-most $p_{\mathrm{T,ch\ jet}}^{\mathrm{reco}}$ region, which is dominated by uncorrelated yield. The value of c_{Ref} is determined from the ratio of the signal and reference TT recoil jet distributions in this region. In Pb–Pb collisions it is found to depend on R and $\Delta\varphi$, with values for $R = 0.2$ of 0.898 ± 0.004 for $\Delta\varphi = \pi/2$ and 0.914 ± 0.008 for $\Delta\varphi = \pi$, and correspondingly 0.751 ± 0.030 and 0.811 ± 0.013 for $R = 0.5$ [23]. In pp collisions it is found to be $\Delta\varphi$ independent, with values of 0.92 and 1.0, for $R = 0.2$ and 0.5, respectively.

In the high-Q^2 partonic scattering regime where QCD factorization is expected to be valid [31], multiple scatterings in the same nuclear collision are independent and do not interfere (multiple-partonic interactions, or MPI). MPI processes which generate a trigger hadron and recoil jet which are in the same event but are uncorrelated constitute a significant background for the search for large-angle jet deflection in this analysis, since the signature of such an effect is a medium-induced change in the $\Delta\varphi$ distribution relative to that in pp collisions, and the MPI-generated distribution is uniform in $\Delta\varphi$, resulting in a $\Delta\varphi$-independent pedestal that masks any $\Delta\varphi$-dependent physical effect. However, as noted above, Eq. (1) corrects the yield due to all uncorrelated sources, including MPIs, and no additional correction procedure to account for the MPI contribution is warranted in the analysis.

After correction for uncorrelated yield (Eq. 1), the resulting Δ_{recoil} distribution is still smeared in both $p_{\mathrm{T,jet}}$ and $\Delta\varphi$ due to detector effects and residual background fluctuations [21, 22]. Correction for this smearing is carried out using iterative Bayesian unfolding [32] in two dimensions ($p_{\mathrm{T,jet}}$, $\Delta\varphi$) when considering Δ_{recoil} as a function of $\Delta\varphi$, and in one dimension ($p_{\mathrm{T,jet}}$) when considering Δ_{recoil} as a function of $p_{\mathrm{T,jet}}$ within $|\Delta\varphi - 0.6| < \pi$. See Ref. [23] for details. The largest systematic uncertainty for pp collisions is due to tracking efficiency, while that for Pb–Pb collisions is due to the choice of prior used for unfolding.

The measurements are compared to several theoretical model calculations incorporating jet quenching. All models considered are Monte Carlo (MC) event generators which utilize PYTHIA8 (Monash tune [33, 34]) to generate hard processes, while differing in treatment of elastic and inelastic jet–medium interactions and the response of the QGP medium. JEWEL [35, 36] calculates the interactions using pQCD matrix elements. JETSCAPE [16] models partonic evolution using MATTER at high virtuality [37, 38] and LBT at low virtuality [39, 40]. The Hybrid Model [41] describes weakly-coupled jet dynamics perturbatively, and strongly-coupled jet–medium interactions with a holographic approach based on the AdS/CFT correspondence. JEWEL calculations are carried out with or without a medium response ("recoils on" or "recoils off"), where for the former the medium response calculation follows the

"4MomSub" prescription [42]. The Hybrid Model optionally includes medium response ("wake") and elastic scattering from discrete scattering centers [19]. Comparison is also made to a leading-order (LO) pQCD calculation with Sudakov resummation, in which medium-induced broadening is controlled by the jet transport coefficient $\hat{q}$ [43].

Figure 1, upper panels, show $\Delta_{\mathrm{recoil}}(p_{\mathrm{T,ch\ jet}})$, the $\Delta_{\mathrm{recoil}}(p_{\mathrm{T,ch\ jet}}, \Delta\varphi)$ distribution integrated over $|\Delta\varphi - \pi| < 0.6$, for $R = 0.2$, 0.4, and 0.5 in pp and central Pb–Pb collisions at $\sqrt{s_{\mathrm{NN}}} = 5.02$ TeV. The distributions cover the range $7 < p_{\mathrm{T,ch\ jet}} < 140$ GeV/c, whose lower limit is the lowest value of $p_{\mathrm{T,jet}}$ reported to date for reconstructed jets measured in heavy-ion collisions at the LHC. The distributions are qualitatively similar, though with shape differences in the region $p_{\mathrm{T,ch\ jet}} \lesssim 30$ GeV/c.
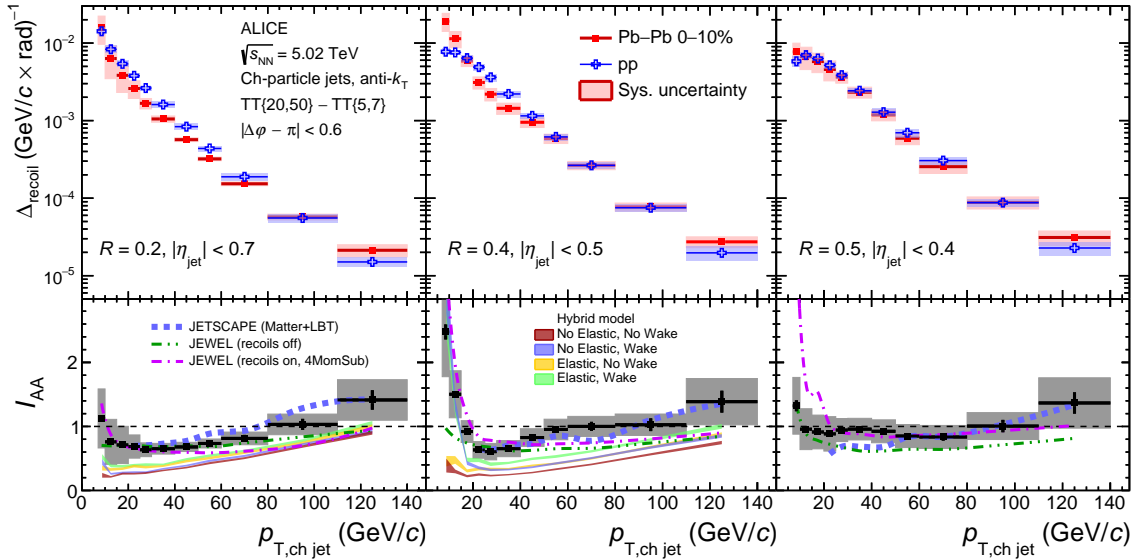
Figure 1: Distributions of recoil jets with $R = 0.2$, 0.4, and 0.5 in pp and central Pb–Pb collisions at $\sqrt{s_{\mathrm{NN}}} = 5.02$ TeV. Upper panels: corrected $\Delta_{\mathrm{recoil}}(p_{\mathrm{T,ch\ jet}})$ distributions. Lower panels: $I_{\mathrm{AA}}(p_{\mathrm{T,ch\ jet}})$ (see text). Also shown are calculations based on JETSCAPE [16], JEWEL [35, 36], and the Hybrid model [41] .

Figure 1, lower panels, show $I_{\mathrm{AA}}(p_{\mathrm{T,ch\ jet}})$, the ratio of the Pb–Pb and pp $\Delta_{\mathrm{recoil}}(p_{\mathrm{T,ch\ jet}})$ distributions. In the range $p_{\mathrm{T,ch\ jet}} < 20$ GeV/c, I_{AA} is consistent with or above unity for all R. For $20 < p_{\mathrm{T,ch\ jet}} \lesssim 60$ GeV/c, I_{AA} is less than unity for $R = 0.2$ and 0.4, indicating yield suppression due to medium-induced energy loss [21]. The value of I_{AA} is consistent with or above unity at higher $p_{\mathrm{T,ch\ jet}}$ for $R = 0.2$ and 0.4, and at all $p_{\mathrm{T,ch\ jet}}$ for $R = 0.5$. An increase in $I_{\mathrm{AA}}(p_{\mathrm{T,ch\ jet}})$ with increasing $p_{\mathrm{T,ch\ jet}}$ may indicate an evolution in the geometric ("surface") bias of vertices which generate the observed high-p_{T} hadron triggers, explored in more detail in Ref. [23]. The $I_{\mathrm{AA}}(p_{\mathrm{T,ch\ jet}})$ distributions for $R = 0.2$ and 0.4 exhibit a broad minimum near $p_{\mathrm{T,ch\ jet}} \sim 20$–30 GeV/$c$, and comparisons with models above and below this minimum are discussed separately.

In the range $p_{\mathrm{T,ch\ jet}} > 20$ GeV/c, for $R = 0.2$ and 0.4 JETSCAPE and the Hybrid Model (all options) exhibit a similar increase in $I_{\mathrm{AA}}(p_{\mathrm{T,ch\ jet}})$ with increasing $p_{\mathrm{T,ch\ jet}}$ as the data. JETSCAPE also reproduces the magnitude of $I_{\mathrm{AA}}(p_{\mathrm{T,ch\ jet}})$, while the Hybrid Model predicts a smaller value. JEWEL (recoils off) agrees with the measured $I_{\mathrm{AA}}(p_{\mathrm{T,ch\ jet}})$ up to 80 GeV/c for $R = 0.2$ and up to 40 GeV/c for $R = 0.4$, but underpredicts it at higher $p_{\mathrm{T,ch\ jet}}$. JEWEL (recoils on) similarly underpredicts the data in $p_{\mathrm{T,ch\ jet}} > 50$ GeV/c. For $R = 0.5$, JETSCAPE describes the data in $p_{\mathrm{T,ch\ jet}} > 50$ GeV/c, but underpredicts it below that range. JEWEL (recoils on) accurately describes the measured I_{AA} in $p_{\mathrm{T,ch\ jet}} > 20$ GeV/c for $R = 0.5$, while JEWEL (recoils off) underpredicts it.

For $p_{T,ch\ jet} < 20$ GeV/c, the data exhibit a marked increase in $I_{AA}(p_{T,ch\ jet})$ with decreasing $p_{T,ch\ jet}$ for $R = 0.4$, with a less significant or negligible increase for $R = 0.2$ and 0.5. Notably, the Hybrid Model with wake-on (both with and without elastic scattering) and JEWEL (recoils on) reproduce the data for $R = 0.4$. This suggests that the increase in $I_{AA}(p_{T,ch\ jet})$ towards low $p_{T,ch\ jet}$ may arise from medium response to interactions of higher-energy jets that are correlated with the trigger; this picture is explored below, after consideration of acoplanarity.
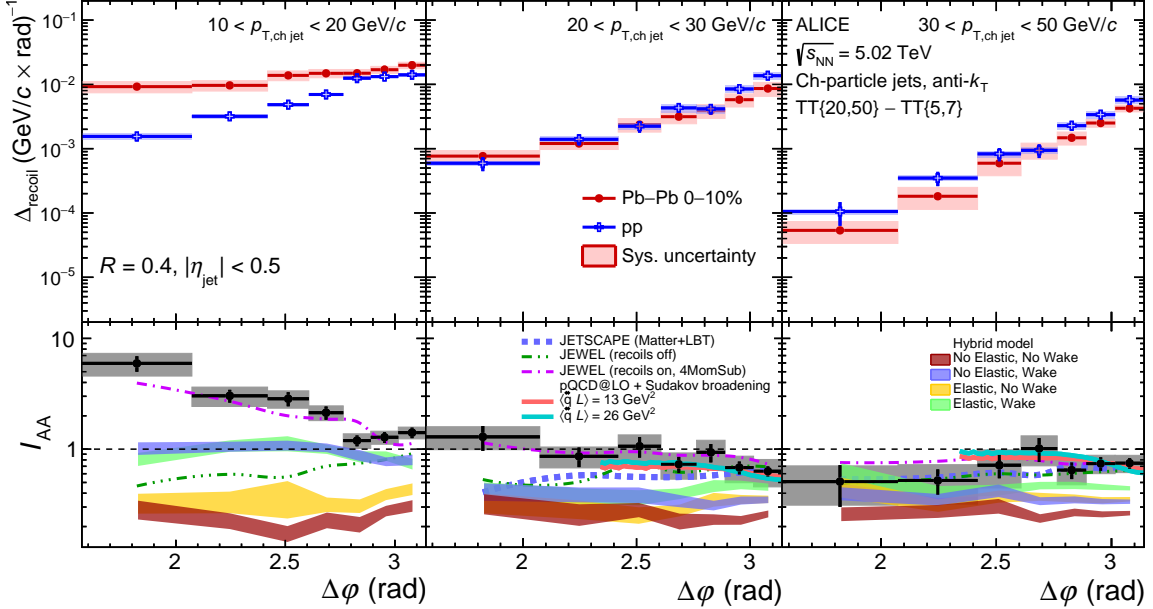
Figure 2: Upper panels: Corrected $\Delta_{recoil}(\Delta\varphi)$ distributions for $R = 0.4$ in Pb–Pb and pp collisions at $\sqrt{s_{NN}} = 5.02$ TeV, for intervals in recoil $p_{T,ch\ jet}$: [10,20] (left), [20,30] (middle), and [30,50] (right) GeV/c. Lower panels: $I_{AA}(\Delta\varphi)$. Predictions from JETSCAPE [16], JEWEL [35, 36], and the LO pQCD calculation [43] are also shown.

Figure 2, upper panels, show $\Delta_{recoil}(\Delta\varphi)$, the $\Delta_{recoil}(p_{T,ch\ jet}, \Delta\varphi)$ distribution projected onto $\Delta\varphi$ in intervals of $p_{T,ch\ jet}$, for $R = 0.4$ in pp and central Pb–Pb collisions. The lower panels show their ratio, $I_{AA}(\Delta\varphi)$. For $30 < p_{T,ch\ jet} < 50$ GeV/c, medium-induced yield suppression ($I_{AA}(\Delta\varphi) < 1$) is observed, largely independent of $\Delta\varphi$. For $20 < p_{T,ch\ jet} < 30$ GeV/c, suppression is observed at $\Delta\varphi \sim \pi$, with a gradual but significant increase of $I_{AA}(\Delta\varphi)$ at larger deviation from $\Delta\varphi \sim \pi$. Notably, for $10 < p_{T,ch\ jet} < 20$ GeV/c, a marked medium-induced excess is observed ($I_{AA}(\Delta\varphi) > 1$), which increases with increasing deviation from $\Delta\varphi \sim \pi$. A linear fit of this distribution in the range $0.5\pi < \Delta\varphi < 0.92\pi$, taking into account uncorrelated uncertainties only, has slope -40.5 ± 8.6, differing by 4.7σ from zero (which corresponds to no medium-induced modification). This is the first observation of strong acoplanarity broadening in the QGP.

Figure 2, lower panels, also show theoretical calculations. The LO pQCD calculation is consistent with the data in the range $20 < p_{T,ch\ jet} < 50$ GeV/c and $2.4 < \Delta\varphi < \pi$ for values of $\langle \hat{q}L \rangle$ between 13 and 26 GeV^2, where L is the in-medium path length. Calculations for a larger range in $\Delta\varphi$, which would provide stronger constraints on $\hat{q}$, require higher perturbative order [44]. JETSCAPE predicts larger suppression than observed in $20 < p_{T,ch\ jet} < 30$ GeV/c, but agrees with the data in the range $30 < p_{T,ch\ jet} < 50$ GeV/c. JEWEL (recoils on) describes both the shape and magnitude of the data well for all $p_{T,ch\ jet}$ intervals, including the significant broadening in $10 < p_{T,ch\ jet} < 20$ GeV/c, which is not captured by JEWEL (recoils off). None of the Hybrid Model variants describes the observed broadening at low $p_{T,ch\ jet}$. These variants generate different magnitude of suppression but underestimate the measured value of I_{AA} in all $p_{T,ch\ jet}$ bins. Only JEWEL (recoils on) correctly reproduces the marked azimuthal

broadening at low $p_{T,ch\ jet}$ seen in data.
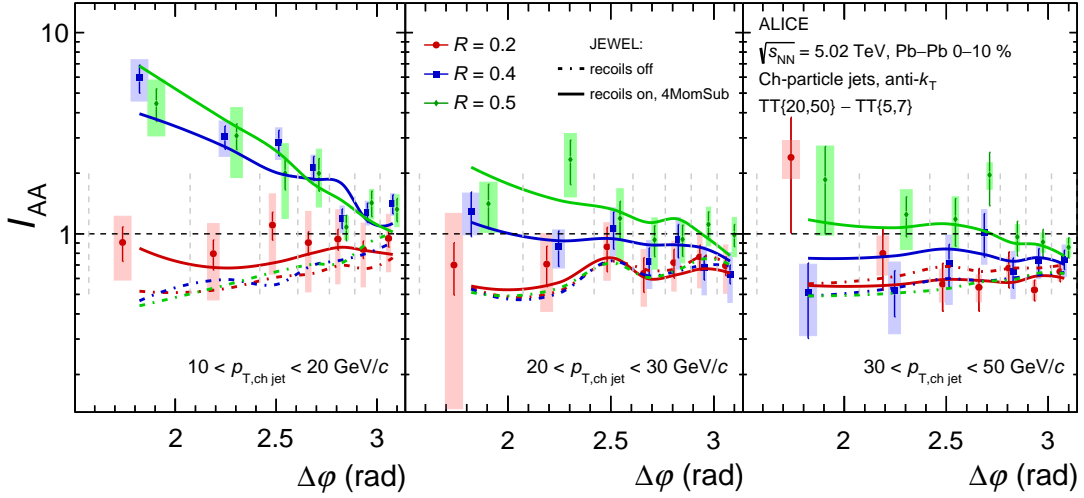
**Figure 3:** $I_{AA}(\Delta\varphi)$ for $R = 0.2$, 0.4 and 0.5, for intervals in recoil $p_{T,ch\ jet}$: [10,20], [20,30], and [30,50] GeV/c. The central points and systematic uncertainties are offset from the center of the $\Delta\varphi$ intervals for clarity. The vertical dashed grey lines represent the $\Delta\varphi$ interval edges. Predictions from JEWEL are also shown.

Figure 3 shows $I_{AA}(\Delta\varphi)$ for $R = 0.2$, 0.4, and 0.5, for the $p_{T,ch\ jet}$ intervals in Fig. 2. The medium-induced acoplanarity broadening in Fig. 2, left panel, is seen only in the range $10 < p_{T,ch\ jet} < 20$ GeV/c, and only for $R = 0.4$ and 0.5 . The value of $I_{AA}(\Delta\varphi)$ is either consistent with unity or suppressed at larger $p_{T,ch\ jet}$ for $R = 0.4$ and 0.5, and for all measured $p_{T,jet}$ for $R = 0.2$. The JEWEL (recoils on) calculation is likewise consistent within uncertainties with all of these data.

Figures 1, 2, and 3 present the first observation of medium-induced jet yield excess and acoplanarity broadening in the QGP. The broadening is significant in the range $10 < p_{T,ch\ jet} < 20$ GeV/c for $R = 0.4$ and 0.5 but is negligible for $R = 0.2$, and is negligible at larger $p_{T,ch\ jet}$ for all R. This rapid transition in the shape of the acoplanarity distribution as a function of both $p_{T,ch\ jet}$ and R is striking. Possible mechanisms that generate acoplanarity broadening include jet scattering from QGP quasi-particles; medium-induced wake effects [45]; and jet splitting, whereby medium-induced radiation from a high-$p_{T,ch\ jet}$ jet is reconstructed at low $p_{T,ch\ jet}$ at large deviation from $\Delta\varphi \sim \pi$.

The latter two mechanisms do not generate perturbatively interpretable jets, and their constituents may be softer in p_T and more diffuse in angle than those of a jet shower in vacuum. In that scenario, the probability for soft and diffuse radiation to mimic a correlated "jet" with $p_{T,ch\ jet} > 10$ GeV/c might scale approximately as the jet area, i.e. as R^2; such scaling could in turn generate a rapid transition in the low $p_{T,ch\ jet}$ enhancement of $I_{AA}(\Delta\varphi)$ between $R = 0.2$ and 0.4/0.5, as observed in data. On the other hand, such a sharp transition is not a natural consequence of jet scattering from QGP quasi-particles, which should generate similar effects for $R = 0.2$, 0.4 and 0.5. The systematic dependence of these measurements on $p_{T,ch\ jet}$ and R therefore disfavors in-medium jet scattering as the primary origin of in-medium acoplanarity broadening. Further measurements, including exploration of the substructure of jets with low $p_{T,ch\ jet}$, can elucidate the contributions of medium response and jet splitting to the observed phenomena.

The low-$p_{T,ch\ jet}$ behavior of $I_{AA}(p_{T,ch\ jet})$ is described both by JEWEL and the Hybrid model, but only if the jet–medium response is included in the simulations. JEWEL (recoils on) also describes $I_{AA}(\Delta\varphi)$ for all R and $p_{T,ch\ jet}$. However, JEWEL (recoils on) does not describe the $p_{T,ch\ jet}$ dependence of $I_{AA}(p_{T,ch\ jet})$ at higher $p_{T,ch\ jet}$ (Fig. 1), and significantly underestimates the suppression of large-R inclu-

sive jets for central Pb–Pb collisions in a similar $p_{\text{T,ch jet}}$ range [13, 46]. None of the models considered here successfully describes all available data.

A measurement of energetic di-jets in Pb–Pb collisions at $\sqrt{s_{\text{NN}}} = 2.76$ TeV has also revealed significant broadening and softening of recoil jet structure [47]. Such measurements, those reported here, and inclusive jet production and jet substructure measurements, probe different aspects of the jet–medium interaction described by model calculations. A global analysis is required for each model, to ascertain whether a fully consistent description of all such data can be achieved by further tuning of model parameters, or whether the jet quenching mechanisms encoded in the model can be excluded by such comparisons to data.

In summary, measurements of semi-inclusive distributions of charged-particle jets recoiling from a high-p_{T} hadron trigger in pp and central Pb–Pb collisions at $\sqrt{s_{\text{NN}}} = 5.02$ TeV have been reported over a broad kinematic range, including low $p_{\text{T,jet}}$ and large R. The ratio of semi-inclusive yields in central Pb–Pb and pp collisions as a function of $p_{\text{T,ch jet}}$, $I_{\text{AA}}(p_{\text{T,ch jet}})$, increases toward large $p_{\text{T,ch jet}}$. This trend is reproduced qualitatively by model calculations incorporating jet quenching. The measurement in this region is influenced by both hadron and jet yield suppression due to energy loss, and provides a new probe of the mechanisms underlying jet quenching.

A marked medium-induced enhancement in recoil jet acoplanarity is observed for the first time for $10 < p_{\text{T,ch jet}} < 20$ GeV/c and large R, with significance 4.7σ relative to no medium-induced modification. The enhancement diminishes rapidly for larger $p_{\text{T,ch jet}}$ and smaller R. These phenomena favor scenarios in which the enhancement arises from the response of the QGP medium to jets or medium-induced jet splitting, and disfavor large-angle jet scattering. These low-$p_{\text{T,ch jet}}$ measurements are well-described by calculations incorporating medium response, which however do not consistently describe the full set of measured data. Further measurements of these phenomena, and their comparison to theoretical calculations, promise significant constraints on the mechanisms governing energy transport and the dynamics of the QGP.

Acknowledgements

References

[1] W. Busza, K. Rajagopal, and W. van der Schee, "Heavy Ion Collisions: The Big Picture, and the Big Questions", *Ann. Rev. Nucl. Part. Sci.* **68** (2018) 339–376, `arXiv:1802.04801 [hep-ph]`.

[2] J. W. Harris and B. Müller, ""QGP Signatures" Revisited", `arXiv:2308.05743 [hep-ph]`.

[3] **BRAHMS** Collaboration, I. Arsene *et al.*, "Quark gluon plasma and color glass condensate at RHIC? The Perspective from the BRAHMS experiment", *Nucl. Phys. A* **757** (2005) 1–27, `arXiv:nucl-ex/0410020`.

[4] **PHENIX** Collaboration, K. Adcox *et al.*, "Formation of dense partonic matter in relativistic nucleus-nucleus collisions at RHIC: Experimental evaluation by the PHENIX collaboration", *Nucl. Phys. A* **757** (2005) 184–283, `arXiv:nucl-ex/0410003`.

[5] **PHOBOS** Collaboration, B. B. Back *et al.*, "The PHOBOS perspective on discoveries at RHIC", *Nucl. Phys. A* **757** (2005) 28–101, `arXiv:nucl-ex/0410022`.

[6] **STAR** Collaboration, J. Adams *et al.*, "Experimental and theoretical challenges in the search for the quark gluon plasma: The STAR Collaboration's critical assessment of the evidence from RHIC collisions", *Nucl. Phys. A* **757** (2005) 102–183, `arXiv:nucl-ex/0501009`.

[7] **ALICE** Collaboration, "The ALICE experiment – A journey through QCD", `arXiv:2211.04384 [nucl-ex]`.

[8] U. Heinz and R. Snellings, "Collective flow and viscosity in relativistic heavy-ion collisions", *Ann. Rev. Nucl. Part. Sci.* **63** (2013) 123–151, `arXiv:1301.2826 [nucl-th]`.

[9] S. Borsanyi, Z. Fodor, C. Hoelbling, S. D. Katz, S. Krieg, and K. K. Szabo, "Full result for the QCD equation of state with 2+1 flavors", *Phys. Lett. B* **730** (2014) 99–104, `arXiv:1309.5258 [hep-lat]`.

[10] **HotQCD** Collaboration, A. Bazavov *et al.*, "Equation of state in (2+1)-flavor QCD", *Phys. Rev. D* **90** (2014) 094503, `arXiv:1407.6387 [hep-lat]`.

[11] **CMS** Collaboration, V. Khachatryan *et al.*, "Measurement of the double-differential inclusive jet cross section in proton–proton collisions at $\sqrt{s} = 13\,\text{TeV}$", *Eur. Phys. J. C* **76** (2016) 451, `arXiv:1605.04436 [hep-ex]`.

[12] **ATLAS** Collaboration, M. Aaboud *et al.*, "Measurement of inclusive jet and dijet cross-sections in proton-proton collisions at $\sqrt{s} = 13$ TeV with the ATLAS detector", *JHEP* **05** (2018) 195, `arXiv:1711.02692 [hep-ex]`.

[13] **ALICE** Collaboration, S. Acharya *et al.*, "Measurements of inclusive jet spectra in pp and central Pb–Pb collisions at $\sqrt{s_{\text{NN}}} = 5.02$ TeV", *Phys. Rev. C* **101** (2020) 034911, `arXiv:1909.09718 [nucl-ex]`.

[14] L. Cunqueiro and A. M. Sickles, "Studying the QGP with Jets at the LHC and RHIC", *Prog. Part. Nucl. Phys.* **124** (2022) 103940, `arXiv:2110.14490 [nucl-ex]`.

[15] A. Majumder and M. Van Leeuwen, "The Theory and Phenomenology of Perturbative QCD Based Jet Quenching", *Prog. Part. Nucl. Phys.* **66** (2011) 41–92, `arXiv:1002.2206 [hep-ph]`.

[16] **JETSCAPE** Collaboration, S. Cao *et al.*, "Determining the jet transport coefficient $\hat{q}$ from inclusive hadron suppression measurements using Bayesian parameter estimation", *Phys. Rev. C* **104** (2021) 024905, `arXiv:2102.11337 [nucl-th]`.

[17] D. A. Appel, "Jets as a Probe of Quark - Gluon Plasmas", *Phys. Rev. D* **33** (1986) 717.

[18] J. P. Blaizot and L. D. McLerran, "Jets in Expanding Quark - Gluon Plasmas", *Phys. Rev. D* **34** (1986) 2739.

[19] F. D'Eramo, K. Rajagopal, and Y. Yin, "Molière scattering in quark-gluon plasma: finding point-like scatterers in a liquid", *JHEP* **01** (2019) 172, `arXiv:1808.03250 [hep-ph]`.

[20] E. Rutherford, "The scattering of alpha and beta particles by matter and the structure of the atom", *Phil. Mag. Ser. 6* **21** (1911) 669–688.

[21] **ALICE** Collaboration, J. Adam *et al.*, "Measurement of jet quenching with semi-inclusive hadron-jet distributions in central Pb–Pb collisions at $\sqrt{s_{\text{NN}}} = 2.76$ TeV", *JHEP* **09** (2015) 170, `arXiv:1506.03984 [nucl-ex]`.

[22] **STAR** Collaboration, L. Adamczyk *et al.*, "Measurements of jet quenching with semi-inclusive hadron+jet distributions in Au+Au collisions at $\sqrt{s_{\text{NN}}} = 200$ GeV", *Phys. Rev. C* **96** (2017) 024905, `arXiv:1702.01108 [nucl-ex]`.

[23] **ALICE** Collaboration, S. Acharya *et al.*, "Measurements of jet quenching using semi-inclusive hadron+jet distributions in pp and central Pb–Pb collisions at $\sqrt{s_{NN}} = 5.02$ TeV ", arXiv:2308.16128 [nucl-ex].

[24] **ALICE** Collaboration, K. Aamodt *et al.*, "The ALICE experiment at the CERN LHC", *JINST* **3** (2008) S08002.

[25] **ALICE** Collaboration, B. Abelev *et al.*, "Performance of the ALICE Experiment at the CERN LHC", *Int. J. Mod. Phys. A* **29** (2014) 1430044, arXiv:1402.4476 [nucl-ex].

[26] http://fastjet.fr/repo/doxygen-3.1.3/.

[27] M. Cacciari, G. P. Salam, and G. Soyez, "The anti-k_t jet clustering algorithm", *JHEP* **04** (2008) 063, arXiv:0802.1189 [hep-ph].

[28] M. Cacciari, G. P. Salam, and G. Soyez, "FastJet User Manual", *Eur. Phys. J. C* **72** (2012) 1896, arXiv:1111.6097 [hep-ph].

[29] M. Cacciari and G. P. Salam, "Pileup subtraction using jet areas", *Phys. Lett. B* **659** (2008) 119–126, arXiv:0707.1378 [hep-ph].

[30] G. O. V. de Barros, B. Fenton-Olsen, P. Jacobs, and M. Ploskon, "Data-driven analysis methods for the measurement of reconstructed jets in heavy ion collisions at RHIC and LHC", *Nucl. Phys. A* **910-911** (2013) 314–318, arXiv:1208.1518 [hep-ex].

[31] J. C. Collins, D. E. Soper, and G. F. Sterman, "Factorization of Hard Processes in QCD", *Adv. Ser. Direct. High Energy Phys.* **5** (1989) 1–91, arXiv:hep-ph/0409313.

[32] T. Adye, "Unfolding algorithms and tests using RooUnfold", in *PHYSTAT 2011*, pp. 313–318. CERN, Geneva, 2011. arXiv:1105.1160 [physics.data-an].

[33] T. Sjöstrand *et al.*, "An introduction to PYTHIA 8.2", *Comput. Phys. Commun.* **191** (2015) 159–177, arXiv:1410.3012 [hep-ph].

[34] P. Skands, S. Carrazza, and J. Rojo, "Tuning PYTHIA 8.1: the Monash 2013 Tune", *Eur. Phys. J. C* **74** (2014) 3024, arXiv:1404.5630 [hep-ph].

[35] K. Zapp, G. Ingelman, J. Rathsman, J. Stachel, and U. A. Wiedemann, "A Monte Carlo Model for 'Jet Quenching'", *Eur. Phys. J. C* **60** (2009) 617–632, arXiv:0804.3568 [hep-ph].

[36] K. C. Zapp, "JEWEL 2.0.0: directions for use", *Eur. Phys. J. C* **74** (2014) 2762, arXiv:1311.0048 [hep-ph].

[37] A. Majumder, "Incorporating Space-Time Within Medium-Modified Jet Event Generators", *Phys. Rev. C* **88** (2013) 014909, arXiv:1301.5323 [nucl-th].

[38] A. Majumder, "The in-medium scale evolution in jet modification", arXiv:0901.4516 [nucl-th].

[39] Y. He, T. Luo, X.-N. Wang, and Y. Zhu, "Linear Boltzmann Transport for Jet Propagation in the Quark-Gluon Plasma: Elastic Processes and Medium Recoil", *Phys. Rev. C* **91** (2015) 054908, arXiv:1503.03313 [nucl-th]. [Erratum: Phys.Rev.C 97, 019902 (2018)].

[40] X.-N. Wang and Y. Zhu, "Medium Modification of γ-jets in High-energy Heavy-ion Collisions", *Phys. Rev. Lett.* **111** (2013) 062301, arXiv:1302.5874 [hep-ph].
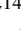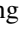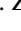
[41] J. Casalderrey-Solana, D. C. Gulhan, J. G. Milhano, D. Pablos, and K. Rajagopal, "A Hybrid Strong/Weak Coupling Approach to Jet Quenching", *JHEP* **10** (2014) 019, arXiv:1405.3864 [hep-ph]. [Erratum: JHEP 09, 175 (2015)].

[42] R. Kunnawalkam Elayavalli and K. C. Zapp, "Medium response in JEWEL and its impact on jet shape observables in heavy ion collisions", *JHEP* **07** (2017) 141, arXiv:1707.01539 [hep-ph].

[43] L. Chen, G.-Y. Qin, S.-Y. Wei, B.-W. Xiao, and H.-Z. Zhang, "Probing Transverse Momentum Broadening via Dihadron and Hadron-jet Angular Correlations in Relativistic Heavy-ion Collisions", *Phys. Lett. B* **773** (2017) 672–676, arXiv:1607.01932 [hep-ph].

[44] L. Chen, G.-Y. Qin, S.-Y. Wei, B.-W. Xiao, and H.-Z. Zhang. Private communication.

[45] S. Cao and X.-N. Wang, "Jet quenching and medium response in high-energy heavy-ion collisions: a review", *Rept. Prog. Phys.* **84** (2021) 024301, arXiv:2002.04028 [hep-ph].

[46] **ALICE** Collaboration, "Measurement of the radius dependence of charged-particle jet suppression in Pb–Pb collisions at $\sqrt{s_{NN}} = 5.02$ TeV", arXiv:2303.00592 [nucl-ex].

[47] **CMS** Collaboration, S. Chatrchyan *et al.*, "Observation and studies of jet quenching in PbPb collisions at nucleon-nucleon center-of-mass energy = 2.76 TeV", *Phys. Rev. C* **84** (2011) 024906, arXiv:1102.1957 [nucl-ex].

W. Guo [6], A. Gupta [91], R. Gupta [91], R. Gupta [48], S.P. Guzman [45], K. Gwizdziel [135], L. Gyulai [138],
C. Hadjidakis [130], F.U. Haider [91], S. Haidlova [36], H. Hamagaki [76], A. Hamdi [74], Y. Han [140],
B.G. Hanley [136], R. Hannigan [108], J. Hansen [75], M.R. Haque [135], J.W. Harris [139], A. Harton [9],
H. Hassan [116], D. Hatzifotiadou [51], P. Hauer [43], L.B. Havener [139], S.T. Heckel [95], E. Hellbär [97],
H. Helstrup [35], M. Hemmer [64], T. Herman [36], G. Herrera Corral [8], F. Herrmann[137], S. Herrmann [127],
K.F. Hetland [35], B. Heybeck [64], H. Hillemanns [33], B. Hippolyte [128], F.W. Hoffmann [70], B. Hofman [59],
G.H. Hong [140], M. Horst [95], A. Horzyk[2], Y. Hou [6], P. Hristov [33], C. Hughes [121], P. Huhn[64],
L.M. Huhta [116], T.J. Humanic [88], A. Hutson [115], D. Hutter [39], R. Ilkaev[142], H. Ilyas [14], M. Inaba [124],
G.M. Innocenti [33], M. Ippolitov [142], A. Isakov [84,86], T. Isidori [117], M.S. Islam [99], M. Ivanov [97],
M. Ivanov[13], V. Ivanov [142], K.E. Iversen [75], M. Jablonski [2], B. Jacak [74], N. Jacazio [26], P.M. Jacobs [74],
S. Jadlovska[106], J. Jadlovsky[106], S. Jaelani [82], C. Jahnke [110], M.J. Jakubowska [135], M.A. Janik [135],
T. Janson[70], S. Ji [17], S. Jia [10], A.A.P. Jimenez [65], F. Jonas [87], D.M. Jones [118], J.M. Jowett [33,97],
J. Jung [64], M. Jung [64], A. Junique [33], A. Jusko [100], M.J. Kabus [33,135], J. Kaewjai[105], P. Kalinak [60],
A.S. Kalteyer [97], A. Kalweit [33], V. Kaplin [142], A. Karasu Uysal [72], D. Karatovic [89], O. Karavichev [142],
T. Karavicheva [142], P. Karczmarczyk [135], E. Karpechev [142], U. Kebschull [70], R. Keidel [141],
D.L.D. Keijdener[59], M. Keil [33], B. Ketzer [43], S.S. Khade [48], A.M. Khan [119], S. Khan [16],
A. Khanzadeev [142], Y. Kharlov [142], A. Khatun [117], A. Khuntia [36], B. Kileng [35], B. Kim [104],
C. Kim [17], D.J. Kim [116], E.J. Kim [69], J. Kim [140], J.S. Kim [41], J. Kim [58], J. Kim [69], M. Kim [19],
S. Kim [18], T. Kim [140], K. Kimura [92], S. Kirsch [64], I. Kisel [39], S. Kiselev [142], A. Kisiel [135],
J.P. Kitowski [2], J.L. Klay [5], J. Klein [33], S. Klein [74], C. Klein-Bösing [137], M. Kleiner [64],
T. Klemenz [95], A. Kluge [33], A.G. Knospe [115], C. Kobdaj [105], T. Kollegger[97], A. Kondratyev [143],
N. Kondratyeva [142], E. Kondratyuk [142], J. Konig [64], S.A. Konigstorfer [95], P.J. Konopka [33],
G. Kornakov [135], S.D. Koryciak [2], A. Kotliarov [86], V. Kovalenko [142], M. Kowalski [107],
V. Kozhuharov [37], I. Králik [60], A. Kravčáková [38], L. Krcal [33,39], M. Krivda [100,60], F. Krizek [86],
K. Krizkova Gajdosova [33], M. Kroesen [94], M. Krüger [64], D.M. Krupova [36], E. Kryshen [142],
V. Kučera [58], C. Kuhn [128], P.G. Kuijer [84], T. Kumaoka[124], D. Kumar[134], L. Kumar [90], N. Kumar[90],
S. Kumar [32], S. Kundu [33], P. Kurashvili [79], A. Kurepin [142], A.B. Kurepin [142], A. Kuryakin [142],
S. Kushpil [86], V. Kuskov[142], M.J. Kweon [58], Y. Kwon [140], S.L. La Pointe [39], P. La Rocca [27],
A. Lakrathok[105], M. Lamanna [33], R. Langoy [120], P. Larionov [33], E. Laudi [33], L. Lautner [33,95],
R. Lavicka [102], R. Lea [133,55], H. Lee [104], I. Legrand [46], G. Legras [137], J. Lehrbach [39], T.M. Lelek[2],
R.C. Lemmon [85], I. León Monzón [109], M.M. Lesch [95], E.D. Lesser [19], P. Lévai [138], X. Li[10],
J. Lien [120], R. Lietava [100], I. Likmeta [115], B. Lim [25], S.H. Lim [17], V. Lindenstruth [39], A. Lindner[46],
C. Lippmann [97], D.H. Liu [6], J. Liu [118], G.S.S. Liveraro [111], I.M. Lofnes [21], C. Loizides [87],
S. Lokos [107], J. Lomker [59], P. Loncar [34], X. Lopez [126], E. López Torres [7], P. Lu [97,119], F.V. Lugo [67],
J.R. Luhder [137], M. Lunardon [28], G. Luparello [57], Y.G. Ma [40], M. Mager [33], A. Maire [128],
M.V. Makariev [37], M. Malaev [142], G. Malfattore [26], N.M. Malik [91], Q.W. Malik[20], S.K. Malik [91],
L. Malinina [VI,143], D. Mallick [130,80], N. Mallick [48], G. Mandaglio [31,53], S.K. Mandal [79], V. Manko [142],
F. Manso [126], V. Manzari [50], Y. Mao [6], R.W. Marcjan [2], G.V. Margagliotti [24], A. Margotti [51],
A. Marín [97], C. Markert [108], P. Martinengo [33], M.I. Martínez [45], G. Martínez García [103],
M.P.P. Martins [110], S. Masciocchi [97], M. Masera [25], A. Masoni [52], L. Massacrier [130], O. Massen [59],
A. Mastroserio [131,50], O. Matonoha [75], S. Mattiazzo [28], A. Matyja [107], C. Mayer [107],
A.L. Mazuecos [33], F. Mazzaschi [25], M. Mazzilli [33], J.E. Mdhluli [122], Y. Melikyan [44],
A. Menchaca-Rocha [67], J.E.M. Mendez [65], E. Meninno [102,29], A.S. Menon [115], M. Meres [13],
S. Mhlanga[113,68], Y. Miake[124], L. Micheletti [33], D.L. Mihaylov [95], K. Mikhaylov [143,142], A.N. Mishra [138],
D. Miśkowiec [97], A. Modak [4], B. Mohanty[80], M. Mohisin Khan[IV,16], M.A. Molander [44], S. Monira [135],
C. Mordasini [116], D.A. Moreira De Godoy [137], I. Morozov [142], A. Morsch [33], T. Mrnjavac [33],
V. Muccifora [49], S. Muhuri [134], J.D. Mulligan [74], A. Mulliri[23], M.G. Munhoz [110], R.H. Munzer [64],
H. Murakami [123], S. Murray [113], L. Musa [33], J. Musinsky [60], J.W. Myrcha [135], B. Naik [122],
A.I. Nambrath [19], B.K. Nandi [47], R. Nania [51], E. Nappi [50], A.F. Nassirpour [18], A. Nath [94],
C. Nattrass [121], M.N. Naydenov [37], A. Neagu[20], A. Negru[125], E. Nekrasova[142], L. Nellen [65],
R. Nepeivoda [75], S. Nese [20], G. Neskovic [39], N. Nicassio [50], B.S. Nielsen [83], E.G. Nielsen [83],
S. Nikolaev [142], S. Nikulin [142], V. Nikulin [142], F. Noferini [51], S. Noh [12], P. Nomokonov [143],
J. Norman [118], N. Novitzky [87], P. Nowakowski [135], A. Nyanin [142], J. Nystrand [21], M. Ogino [76],
S. Oh [18], A. Ohlson [75], V.A. Okorokov [142], J. Oleniacz [135], A.C. Oliveira Da Silva [121],
A. Onnerstad [116], C. Oppedisano [56], A. Ortiz Velasquez [65], J. Otwinowski [107], M. Oya[92], K. Oyama [76],
Y. Pachmayer [94], S. Padhan [47], D. Pagano [133,55], G. Paić [65], A. Palasciano [50], S. Panebianco [129],

H. Park [124], H. Park [104], J. Park [58], J.E. Parkkila [33], Y. Patley [47], R.N. Patra[91], B. Paul [23], H. Pei [6], T. Peitzmann [59], X. Peng [11], M. Pennisi [25], S. Perciballi [25], D. Peresunko [142], G.M. Perez [7], Y. Pestov[142], V. Petrov [142], M. Petrovici [46], R.P. Pezzi [103,66], S. Piano [57], M. Pikna [13], P. Pillot [103], O. Pinazza [51,33], L. Pinsky[115], C. Pinto [95], S. Pisano [49], M. Płoskoń [74], M. Planinic[89], F. Pliquett[64], M.G. Poghosyan [87], B. Polichtchouk [142], S. Politano [30], N. Poljak [89], A. Pop [46], S. Porteboeuf-Houssais [126], V. Pozdniakov [143], I.Y. Pozos [45], K.K. Pradhan [48], S.K. Prasad [4], S. Prasad [48], R. Preghenella [51], F. Prino [56], C.A. Pruneau [136], I. Pshenichnov [142], M. Puccio [33], S. Pucillo [25], Z. Pugelova[106], S. Qiu [84], L. Quaglia [25], S. Ragoni [15], A. Rai [139], A. Rakotozafindrabe [129], L. Ramello [132,56], F. Rami [128], S.A.R. Ramirez [45], T.A. Rancien[73], M. Rasa [27], S.S. Räsänen [44], R. Rath [51], M.P. Rauch [21], I. Ravasenga [84], K.F. Read [87,121], C. Reckziegel [112], A.R. Redelbach [39], K. Redlich [V,79], C.A. Reetz [97], A. Rehman[21], F. Reidt [33], H.A. Reme-Ness [35], Z. Rescakova[38], K. Reygers [94], A. Riabov [142], V. Riabov [142], R. Ricci [29], M. Richter [20], A.A. Riedel [95], W. Riegler [33], A.G. Riffero [25], C. Ristea [63], M.V. Rodriguez [33], M. Rodríguez Cahuantzi [45], K. Røed [20], R. Rogalev [142], E. Rogochaya [143], T.S. Rogoschinski [64], D. Rohr [33], D. Röhrich [21], P.F. Rojas[45], S. Rojas Torres [36], P.S. Rokita [135], G. Romanenko [26], F. Ronchetti [49], A. Rosano [31,53], E.D. Rosas[65], K. Roslon [135], A. Rossi [54], A. Roy [48], S. Roy [47], N. Rubini [26], D. Ruggiano [135], R. Rui [24], P.G. Russek [2], R. Russo [84], A. Rustamov [81], E. Ryabinkin [142], Y. Ryabov [142], A. Rybicki [107], H. Rytkonen [116], J. Ryu [17], W. Rzesa [135], O.A.M. Saarimaki [44], S. Sadhu [32], S. Sadovsky [142], J. Saetre [21], K. Šafařík [36], P. Saha[42], S.K. Saha [4], S. Saha [80], B. Sahoo [47], B. Sahoo [48], R. Sahoo [48], S. Sahoo[61], D. Sahu [48], P.K. Sahu [61], J. Saini [134], K. Sajdakova[38], S. Sakai [124], M.P. Salvan [97], S. Sambyal [91], D. Samitz [102], I. Sanna [33,95], T.B. Saramela[110], P. Sarma [42], V. Sarritzu [23], V.M. Sarti [95], M.H.P. Sas [33], S. Sawan[80], J. Schambach [87], H.S. Scheid [64], C. Schiaua [46], R. Schicker [94], F. Schlepper [94], A. Schmah[97], C. Schmidt [97], H.R. Schmidt[93], M.O. Schmidt [33], M. Schmidt[93], N.V. Schmidt [87], A.R. Schmier [121], R. Schotter [128], A. Schröter [39], J. Schukraft [33], K. Schweda [97], G. Scioli [26], E. Scomparin [56], J.E. Seger [15], Y. Sekiguchi[123], D. Sekihata [123], M. Selina [84], I. Selyuzhenkov [97], S. Senyukov [128], J.J. Seo [94,58], D. Serebryakov [142], L. Šerkšnytė [95], A. Sevcenco [63], T.J. Shaba [68], A. Shabetai [103], R. Shahoyan[33], A. Shangaraev [142], A. Sharma[90], B. Sharma [91], D. Sharma [47], H. Sharma [54], M. Sharma [91], S. Sharma [76], S. Sharma [91], U. Sharma [91], A. Shatat [130], O. Sheibani[115], K. Shigaki [92], M. Shimomura[77], J. Shin[12], S. Shirinkin [142], Q. Shou [40], Y. Sibiriak [142], S. Siddhanta [52], T. Siemiarczuk [79], T.F. Silva [110], D. Silvermyr [75], T. Simantathammakul[105], R. Simeonov [37], B. Singh[91], B. Singh [95], K. Singh [48], R. Singh [80], R. Singh [91], R. Singh [48], S. Singh [16], V.K. Singh [134], V. Singhal [134], T. Sinha [99], B. Sitar [13], M. Sitta [132,56], T.B. Skaali[20], G. Skorodumovs [94], M. Slupecki [44], N. Smirnov [139], R.J.M. Snellings [59], E.H. Solheim [20], J. Song [17], C. Sonnabend [33,97], F. Soramel [28], A.B. Soto-hernandez [88], R. Spijkers [84], I. Sputowska [107], J. Staa [75], J. Stachel [94], I. Stan [63], P.J. Steffanic [121], S.F. Stiefelmaier [94], D. Stocco [103], I. Storehaug [20], P. Stratmann [137], S. Strazzi [26], A. Sturniolo [31,53], C.P. Stylianidis[84], A.A.P. Suaide [110], C. Suire [130], M. Sukhanov [142], M. Suljic [33], R. Sultanov [142], V. Sumberia [91], S. Sumowidagdo [82], S. Swain[61], I. Szarka [13], M. Szymkowski [135], S.F. Taghavi [95], G. Taillepied [97], J. Takahashi [111], G.J. Tambave [80], S. Tang [6], Z. Tang [119], J.D. Tapia Takaki [117], N. Tapus[125], L.A. Tarasovicova [137], M.G. Tarzila [46], G.F. Tassielli [32], A. Tauro [33], G. Tejeda Muñoz [45], A. Telesca [33], L. Terlizzi [25], C. Terrevoli [115], S. Thakur [4], D. Thomas [108], A. Tikhonov [142], N. Tiltmann [33,137], A.R. Timmins [115], M. Tkacik[106], T. Tkacik [106], A. Toia [64], R. Tokumoto[92], K. Tomohiro[92], N. Topilskaya [142], M. Toppi [49], T. Tork [130], P.V. Torres[65], V.V. Torres [103], A.G. Torres Ramos [32], A. Trifiró [31,53], A.S. Triolo [33,31,53], S. Tripathy [51], T. Tripathy [47], S. Trogolo [33], V. Trubnikov [3], W.H. Trzaska [116], T.P. Trzcinski [135], A. Tumkin [142], R. Turrisi [54], T.S. Tveter [20], K. Ullaland [21], B. Ulukutlu [95], A. Uras [127], G.L. Usai [23], M. Vala[38], N. Valle [22], L.V.R. van Doremalen[59], M. van Leeuwen [84], C.A. van Veen [94], R.J.G. van Weelden [84], P. Vande Vyvre [33], D. Varga [138], Z. Varga [138], M. Vasileiou [78], A. Vasiliev [142], O. Vázquez Doce [49], O. Vazquez Rueda [115], V. Vechernin [142], E. Vercellin [25], S. Vergara Limón[45], R. Verma[47], L. Vermunt [97], R. Vértesi [138], M. Verweij [59], L. Vickovic[34], Z. Vilakazi[122], O. Villalobos Baillie [100], A. Villani [24], A. Vinogradov [142], T. Virgili [29], M.M.O. Virta [116], V. Vislavicius[75], A. Vodopyanov [143], B. Volkel [33], M.A. Völkl [94], K. Voloshin[142], S.A. Voloshin [136], G. Volpe [32], B. von Haller [33], I. Vorobyev [95], N. Vozniuk [142], J. Vrláková [38], J. Wan[40], C. Wang [40], D. Wang[40], Y. Wang [40], Y. Wang [6], A. Wegrzynek [33], F.T. Weiglhofer[39], S.C. Wenzel [33], J.P. Wessels [137], S.L. Weyhmiller [139], J. Wiechula [64], J. Wikne [20], G. Wilk [79], J. Wilkinson [97], G.A. Willems [137], B. Windelband [94], M. Winn [129], J.R. Wright [108], W. Wu[40], Y. Wu [119], R. Xu [6], A. Yadav [43], A.K. Yadav [134],

S. Yalcin [72], Y. Yamaguchi [92], S. Yang[21], S. Yano [92], Z. Yin [6], I.-K. Yoo [17], J.H. Yoon [58], H. Yu[12], S. Yuan[21], A. Yuncu [94], V. Zaccolo [24], C. Zampolli [33], F. Zanone [94], N. Zardoshti [33], A. Zarochentsev [142], P. Závada [62], N. Zaviyalov[142], M. Zhalov [142], B. Zhang [6], C. Zhang [129], L. Zhang [40], S. Zhang [40], X. Zhang [6], Y. Zhang[119], Z. Zhang [6], M. Zhao [10], V. Zherebchevskii [142], Y. Zhi[10], D. Zhou [6], Y. Zhou [83], J. Zhu [97,6], Y. Zhu[6], S.C. Zugravel [56], N. Zurlo [133,55]

Affiliation Notes

[I] Also at: Max-Planck-Institut für Physik, Munich, Germany
[II] Also at: Italian National Agency for New Technologies, Energy and Sustainable Economic Development (ENEA), Bologna, Italy
[III] Also at: Dipartimento DET del Politecnico di Torino, Turin, Italy
[IV] Also at: Department of Applied Physics, Aligarh Muslim University, Aligarh, India
[V] Also at: Institute of Theoretical Physics, University of Wroclaw, Poland
[VI] Also at: An institution covered by a cooperation agreement with CERN

Collaboration Institutes

[1] A.I. Alikhanyan National Science Laboratory (Yerevan Physics Institute) Foundation, Yerevan, Armenia
[2] AGH University of Krakow, Cracow, Poland
[3] Bogolyubov Institute for Theoretical Physics, National Academy of Sciences of Ukraine, Kiev, Ukraine
[4] Bose Institute, Department of Physics and Centre for Astroparticle Physics and Space Science (CAPSS), Kolkata, India
[5] California Polytechnic State University, San Luis Obispo, California, United States
[6] Central China Normal University, Wuhan, China
[7] Centro de Aplicaciones Tecnológicas y Desarrollo Nuclear (CEADEN), Havana, Cuba
[8] Centro de Investigación y de Estudios Avanzados (CINVESTAV), Mexico City and Mérida, Mexico
[9] Chicago State University, Chicago, Illinois, United States
[10] China Institute of Atomic Energy, Beijing, China
[11] China University of Geosciences, Wuhan, China
[12] Chungbuk National University, Cheongju, Republic of Korea
[13] Comenius University Bratislava, Faculty of Mathematics, Physics and Informatics, Bratislava, Slovak Republic
[14] COMSATS University Islamabad, Islamabad, Pakistan
[15] Creighton University, Omaha, Nebraska, United States
[16] Department of Physics, Aligarh Muslim University, Aligarh, India
[17] Department of Physics, Pusan National University, Pusan, Republic of Korea
[18] Department of Physics, Sejong University, Seoul, Republic of Korea
[19] Department of Physics, University of California, Berkeley, California, United States
[20] Department of Physics, University of Oslo, Oslo, Norway
[21] Department of Physics and Technology, University of Bergen, Bergen, Norway
[22] Dipartimento di Fisica, Università di Pavia, Pavia, Italy
[23] Dipartimento di Fisica dell'Università and Sezione INFN, Cagliari, Italy
[24] Dipartimento di Fisica dell'Università and Sezione INFN, Trieste, Italy
[25] Dipartimento di Fisica dell'Università and Sezione INFN, Turin, Italy
[26] Dipartimento di Fisica e Astronomia dell'Università and Sezione INFN, Bologna, Italy
[27] Dipartimento di Fisica e Astronomia dell'Università and Sezione INFN, Catania, Italy
[28] Dipartimento di Fisica e Astronomia dell'Università and Sezione INFN, Padova, Italy
[29] Dipartimento di Fisica 'E.R. Caianiello' dell'Università and Gruppo Collegato INFN, Salerno, Italy
[30] Dipartimento DISAT del Politecnico and Sezione INFN, Turin, Italy
[31] Dipartimento di Scienze MIFT, Università di Messina, Messina, Italy
[32] Dipartimento Interateneo di Fisica 'M. Merlin' and Sezione INFN, Bari, Italy
[33] European Organization for Nuclear Research (CERN), Geneva, Switzerland
[34] Faculty of Electrical Engineering, Mechanical Engineering and Naval Architecture, University of Split, Split, Croatia
[35] Faculty of Engineering and Science, Western Norway University of Applied Sciences, Bergen, Norway

[36] Faculty of Nuclear Sciences and Physical Engineering, Czech Technical University in Prague, Prague, Czech Republic

[37] Faculty of Physics, Sofia University, Sofia, Bulgaria

[38] Faculty of Science, P.J. Šafárik University, Košice, Slovak Republic

[39] Frankfurt Institute for Advanced Studies, Johann Wolfgang Goethe-Universität Frankfurt, Frankfurt, Germany

[40] Fudan University, Shanghai, China

[41] Gangneung-Wonju National University, Gangneung, Republic of Korea

[42] Gauhati University, Department of Physics, Guwahati, India

[43] Helmholtz-Institut für Strahlen- und Kernphysik, Rheinische Friedrich-Wilhelms-Universität Bonn, Bonn, Germany

[44] Helsinki Institute of Physics (HIP), Helsinki, Finland

[45] High Energy Physics Group, Universidad Autónoma de Puebla, Puebla, Mexico

[46] Horia Hulubei National Institute of Physics and Nuclear Engineering, Bucharest, Romania

[47] Indian Institute of Technology Bombay (IIT), Mumbai, India

[48] Indian Institute of Technology Indore, Indore, India

[49] INFN, Laboratori Nazionali di Frascati, Frascati, Italy

[50] INFN, Sezione di Bari, Bari, Italy

[51] INFN, Sezione di Bologna, Bologna, Italy

[52] INFN, Sezione di Cagliari, Cagliari, Italy

[53] INFN, Sezione di Catania, Catania, Italy

[54] INFN, Sezione di Padova, Padova, Italy

[55] INFN, Sezione di Pavia, Pavia, Italy

[56] INFN, Sezione di Torino, Turin, Italy

[57] INFN, Sezione di Trieste, Trieste, Italy

[58] Inha University, Incheon, Republic of Korea

[59] Institute for Gravitational and Subatomic Physics (GRASP), Utrecht University/Nikhef, Utrecht, Netherlands

[60] Institute of Experimental Physics, Slovak Academy of Sciences, Košice, Slovak Republic

[61] Institute of Physics, Homi Bhabha National Institute, Bhubaneswar, India

[62] Institute of Physics of the Czech Academy of Sciences, Prague, Czech Republic

[63] Institute of Space Science (ISS), Bucharest, Romania

[64] Institut für Kernphysik, Johann Wolfgang Goethe-Universität Frankfurt, Frankfurt, Germany

[65] Instituto de Ciencias Nucleares, Universidad Nacional Autónoma de México, Mexico City, Mexico

[66] Instituto de Física, Universidade Federal do Rio Grande do Sul (UFRGS), Porto Alegre, Brazil

[67] Instituto de Física, Universidad Nacional Autónoma de México, Mexico City, Mexico

[68] iThemba LABS, National Research Foundation, Somerset West, South Africa

[69] Jeonbuk National University, Jeonju, Republic of Korea

[70] Johann-Wolfgang-Goethe Universität Frankfurt Institut für Informatik, Fachbereich Informatik und Mathematik, Frankfurt, Germany

[71] Korea Institute of Science and Technology Information, Daejeon, Republic of Korea

[72] KTO Karatay University, Konya, Turkey

[73] Laboratoire de Physique Subatomique et de Cosmologie, Université Grenoble-Alpes, CNRS-IN2P3, Grenoble, France

[74] Lawrence Berkeley National Laboratory, Berkeley, California, United States

[75] Lund University Department of Physics, Division of Particle Physics, Lund, Sweden

[76] Nagasaki Institute of Applied Science, Nagasaki, Japan

[77] Nara Women's University (NWU), Nara, Japan

[78] National and Kapodistrian University of Athens, School of Science, Department of Physics , Athens, Greece

[79] National Centre for Nuclear Research, Warsaw, Poland

[80] National Institute of Science Education and Research, Homi Bhabha National Institute, Jatni, India

[81] National Nuclear Research Center, Baku, Azerbaijan

[82] National Research and Innovation Agency - BRIN, Jakarta, Indonesia

[83] Niels Bohr Institute, University of Copenhagen, Copenhagen, Denmark

[84] Nikhef, National institute for subatomic physics, Amsterdam, Netherlands

[85] Nuclear Physics Group, STFC Daresbury Laboratory, Daresbury, United Kingdom

[86] Nuclear Physics Institute of the Czech Academy of Sciences, Husinec-Řež, Czech Republic

[87] Oak Ridge National Laboratory, Oak Ridge, Tennessee, United States

[88] Ohio State University, Columbus, Ohio, United States

[89] Physics department, Faculty of science, University of Zagreb, Zagreb, Croatia

[90] Physics Department, Panjab University, Chandigarh, India

[91] Physics Department, University of Jammu, Jammu, India

[92] Physics Program and International Institute for Sustainability with Knotted Chiral Meta Matter (SKCM2), Hiroshima University, Hiroshima, Japan

[93] Physikalisches Institut, Eberhard-Karls-Universität Tübingen, Tübingen, Germany

[94] Physikalisches Institut, Ruprecht-Karls-Universität Heidelberg, Heidelberg, Germany

[95] Physik Department, Technische Universität München, Munich, Germany

[96] Politecnico di Bari and Sezione INFN, Bari, Italy

[97] Research Division and ExtreMe Matter Institute EMMI, GSI Helmholtzzentrum für Schwerionenforschung GmbH, Darmstadt, Germany

[98] Saga University, Saga, Japan

[99] Saha Institute of Nuclear Physics, Homi Bhabha National Institute, Kolkata, India

[100] School of Physics and Astronomy, University of Birmingham, Birmingham, United Kingdom

[101] Sección Física, Departamento de Ciencias, Pontificia Universidad Católica del Perú, Lima, Peru

[102] Stefan Meyer Institut für Subatomare Physik (SMI), Vienna, Austria

[103] SUBATECH, IMT Atlantique, Nantes Université, CNRS-IN2P3, Nantes, France

[104] Sungkyunkwan University, Suwon City, Republic of Korea

[105] Suranaree University of Technology, Nakhon Ratchasima, Thailand

[106] Technical University of Košice, Košice, Slovak Republic

[107] The Henryk Niewodniczanski Institute of Nuclear Physics, Polish Academy of Sciences, Cracow, Poland

[108] The University of Texas at Austin, Austin, Texas, United States

[109] Universidad Autónoma de Sinaloa, Culiacán, Mexico

[110] Universidade de São Paulo (USP), São Paulo, Brazil

[111] Universidade Estadual de Campinas (UNICAMP), Campinas, Brazil

[112] Universidade Federal do ABC, Santo Andre, Brazil

[113] University of Cape Town, Cape Town, South Africa

[114] University of Derby, Derby, United Kingdom

[115] University of Houston, Houston, Texas, United States

[116] University of Jyväskylä, Jyväskylä, Finland

[117] University of Kansas, Lawrence, Kansas, United States

[118] University of Liverpool, Liverpool, United Kingdom

[119] University of Science and Technology of China, Hefei, China

[120] University of South-Eastern Norway, Kongsberg, Norway

[121] University of Tennessee, Knoxville, Tennessee, United States

[122] University of the Witwatersrand, Johannesburg, South Africa

[123] University of Tokyo, Tokyo, Japan

[124] University of Tsukuba, Tsukuba, Japan

[125] University Politehnica of Bucharest, Bucharest, Romania

[126] Université Clermont Auvergne, CNRS/IN2P3, LPC, Clermont-Ferrand, France

[127] Université de Lyon, CNRS/IN2P3, Institut de Physique des 2 Infinis de Lyon, Lyon, France

[128] Université de Strasbourg, CNRS, IPHC UMR 7178, F-67000 Strasbourg, France, Strasbourg, France

[129] Université Paris-Saclay, Centre d'Etudes de Saclay (CEA), IRFU, Départent de Physique Nucléaire (DPhN), Saclay, France

[130] Université Paris-Saclay, CNRS/IN2P3, IJCLab, Orsay, France

[131] Università degli Studi di Foggia, Foggia, Italy

[132] Università del Piemonte Orientale, Vercelli, Italy

[133] Università di Brescia, Brescia, Italy

[134] Variable Energy Cyclotron Centre, Homi Bhabha National Institute, Kolkata, India

[135] Warsaw University of Technology, Warsaw, Poland

[136] Wayne State University, Detroit, Michigan, United States

[137] Westfälische Wilhelms-Universität Münster, Institut für Kernphysik, Münster, Germany

[138] Wigner Research Centre for Physics, Budapest, Hungary

[139] Yale University, New Haven, Connecticut, United States

[140] Yonsei University, Seoul, Republic of Korea

[141] Zentrum für Technologie und Transfer (ZTT), Worms, Germany

[142] Affiliated with an institute covered by a cooperation agreement with CERN

[143] Affiliated with an international laboratory covered by a cooperation agreement with CERN.